



**UNIVERSITY OF LEEDS**

This is a repository copy of *Quiet power-free cooling system enabled by loop heat pipe*.

White Rose Research Online URL for this paper:

<http://eprints.whiterose.ac.uk/155097/>

Version: Accepted Version

---

**Article:**

Bai, L, Fu, J, Lin, G et al. (2 more authors) (2019) Quiet power-free cooling system enabled by loop heat pipe. *Applied Thermal Engineering*, 155. pp. 14-23. ISSN 1359-4311

<https://doi.org/10.1016/j.applthermaleng.2019.03.147>

---

© 2019 Elsevier Ltd. All rights reserved. This manuscript version is made available under the CC-BY-NC-ND 4.0 license <http://creativecommons.org/licenses/by-nc-nd/4.0/>.

**Reuse**

This article is distributed under the terms of the Creative Commons Attribution-NonCommercial-NoDerivs (CC BY-NC-ND) licence. This licence only allows you to download this work and share it with others as long as you credit the authors, but you can't change the article in any way or use it commercially. More information and the full terms of the licence here: <https://creativecommons.org/licenses/>

**Takedown**

If you consider content in White Rose Research Online to be in breach of UK law, please notify us by emailing [eprints@whiterose.ac.uk](mailto:eprints@whiterose.ac.uk) including the URL of the record and the reason for the withdrawal request.



[eprints@whiterose.ac.uk](mailto:eprints@whiterose.ac.uk)  
<https://eprints.whiterose.ac.uk/>

# Quiet power-free cooling system enabled by loop heat pipe

Lizhan Bai<sup>1,\*</sup>, Jingwei Fu<sup>1</sup>, Guiping Lin<sup>1</sup>, Chengshuang Zhou<sup>2</sup>, Dongsheng Wen<sup>1, 3</sup>

<sup>1</sup> Laboratory of Fundamental Science on Ergonomics and Environmental Control, School of Aeronautic Science and Engineering,

Beihang University, Beijing 100191, PR China

<sup>2</sup> College of Materials Science and Engineering, Zhejiang University of Technology, Hangzhou 310014, PR China

<sup>3</sup> School of Chemical and Process Engineering, University of Leeds, Leeds, LS2 9JT, UK

**Abstract:** Loop heat pipe (LHP) is a quite promising two-phase heat transfer device, holding significant application potential in the modern electronics cooling. In this work, a LHP-based cooling system has been developed, which features no power consumption and no noise, taking full advantage of LHP's efficient long-distance heat transport capability. The heat source was simulated by a film electric resistance heater, which was connected to the cylindrical evaporator of the LHP through an aluminum saddle. The condenser line was embedded into the bottom surface of a fin radiator with a relatively large volume, where heat dissipation to the ambient was completely in the form of air natural convection. Extensive experiments on this cooling system were conducted, mainly focusing on its startup and system thermal resistance. Experimental results show that this cooling system can successfully realize the startup with a very small heat load. With the film heater temperature not exceeding 80 °C, this cooling system can dissipate a heat load up to 150 W to the ambient at a temperature about 24 °C, corresponding to a system thermal resistance about 0.30 °C/W. In addition, this cooling system exhibited very strong anti-gravity capability. With an adverse elevation of 0.5 m, the cooling system can realize normal operation, and no obvious performance decay was observed except an increased operating temperature at small heat loads.

**Keywords:** loop heat pipe; cooling; startup; heat transfer; experiment

## **1 Introduction**

With the rapid development of modern electronic and telecommunication industry, electronics cooling is increasingly becoming an issue to be resolved, and sometimes even a bottleneck restricting the further development of device miniaturization and/or power upgrade [1-3]. That is because electronics cooling is of great importance in maintaining the normal operation of the electronic devices and modules, especially when the power density is relatively large. With the increase of the operating temperature, both the operating performance and reliability of electronic devices decrease; and once the device temperature exceeds its maximum allowable value, an operation failure will occur. In particular, at very high temperatures even a burn-out may happen, causing serious unexpected accidents. As the heat generated from the electronic devices keeps an ever-growing trend, it continuously imposes new challenge to the cooling technology.

Traditional electronics cooling methods mainly include air natural convection, air forced convection, and liquid cooling through conventional or micro channels. Air natural convection consumes no power, but it is only applicable when the heat generated is very small, such as the cooling of power cable, desktop monitor and smart phone. For air forced convection, it is the most popular cooling technology, which is widespread in the cooling of the CPU of the desktops. A fan or blower is needed where a certain power consumption is necessary, and its cooling capacity is intermediate. When the cooling capacity is relatively large, large noise may be produced from this cooling system, due to considerably increased wind quantity per unit time. Liquid cooling refers to cooling by means of the circulation of a liquid coolant. Because the thermal conductivity and heat capacity of liquid are generally far larger than those of air, the cooling capacity for liquid cooling can be very large. Especially when the micro channels are employed, liquid cooling can become a very efficient cooling technology [4-5]. However, for a liquid cooling system, a pump is indispensable to circulate the working fluid, and a fan is also required to dissipate the heat absorbed by the liquid to the ambient eventually. In addition, possible liquid leakage also presents a risk, and sealing and pump lifespan are the mainly two concerns for this system.

To address the increasingly severe cooling issue, various heat pipe-integrated cooling systems have been developed and studied recently [6-7]. Xiao et al. proposed a U-shaped heat pipe cooling system with a fan to solve the thermal management problem of high-power LEDs [8]. With increased airflow rate produced by the fan, the thermal performance of the system can be improved significantly, having the advantages of strong cooling capacity, simple structure and easy installation. The experimental results showed that the substrate temperature could maintain as low as 25 °C when the combination of the heat pipe and fan was adopted. As long as the proper ambient temperature and air flowrate were available, the LED junction temperature can be well controlled. Weng et al. experimentally studied the heat pipes with phase change materials for electronic device cooling [9]. A storage container containing a phase change material on the heat pipe can store and release the thermal energy. Compared with conventional heat pipes without heat storage materials, the heat pipe module with tricosane as PCM cooling module could save 46% of fan power consumption, and reduce the heater temperature by an average of 12.3°C. Tran et al. used heat pipes for the cooling of lithium-ion batteries of hybrid and electric vehicles [10]. The heat pipe was coupled to the confined ventilation structure to maintain the battery temperature within an optimum range and uniform the temperature distribution. The study found that the association of heat pipe cooling with chimney ventilation can significantly improve the heat rejection without any power consumption.

For the current heat pipe-integrated cooling system, it possesses excellent cooling performance and thus receives wide applications. However, it is only applicable when the cooling space is very adjacent to the heat source, and the heat pipe evaporator must be installed horizontal with or lower than its condenser. Because for conventional heat pipe, its long distance heat transport capability is not strong, caused by its inherent structural characters such as the arrangement of the microporous wick throughout the body. At the same time, the anti-gravity operation will also cause severe performance degradation to this system due to insufficient liquid supply to replenish the evaporator wick. In the case to overcome long distance heat transport and anti-gravity operation, the employment of a loop heat pipe (LHP) is a perfect

choice. Its long distance heat transport capability and flexibility in design as well as strong antigravity capability could offer many advantages compared with traditional heat pipes.

Currently, LHP has been applied in the spacecraft thermal control systems to address the time-varying thermal management problems during the whole mission where great success has been achieved [11-15]. Following the success in the field of space thermal control, to expand LHP applications to the ground environment seems logical, and great efforts have been made by quite a few researchers worldwide, as briefly reviewed below. Pastukhov et al. developed miniature loop heat pipes (mLHPs) with a nominal capacity of 25-30 W and a heat-transfer distance up to 250 mm for cooling electronic components and CPU of mobile PC [16]. Several prototypes of mLHPs with the evaporator diameters no more than 6 mm and ammonia as the working fluid were incorporated into remote heat exchanger (RHE) systems in different conditions. Under air forced cooling the total thermal resistance of such a system is 1.7-4.0 °C/W and depends strongly on the cooling conditions and the radiator efficiency. Based on the experimental results, mLHPs can be regarded as quite promising devices for RHE systems providing efficient cooling for electronics components and personal computers.

In order to decrease the noise level created at the operation of cooling system fans, Pastukhov et al. proposed to create a passive or semi-passive systems on the base of LHPs in which the heat sink is an external radiator cooled by natural or forced air convection [17]. The LHP-based cooling system developed was capable of sustaining an operating temperature of 72-78 °C on the heat source thermal interface which dissipated a heat load of 100 W at an ambient temperature of 22 °C. It is also shown that the use of additional means of active cooling in combination with LHPs allows to increase the value of dissipated heat up to 180 W and to decrease the system thermal resistance down to 0.29 °C/W. Zhou et al., fabricated a miniature loop heat pipe (mLHP) employing a 1.2 mm thick flat evaporator and a vapor line, liquid line and condenser with a 1.0 mm thickness, for cooling mobile electronics [18]. The mLHP employed an internal wick structure fabricated of sintered fine copper mesh, comprised of a primary

wick structure in the evaporator to provide the driving force for circulating the working fluid, and a secondary wick inside the liquid line to promote the flow of condensed working fluid back to the evaporator. The proposed mLHP demonstrated stable start-up behavior at a low heat load of 2 W in the horizontal orientation with an evaporator temperature of 43.9 °C and efficiently dissipated a maximum heat load of 12 W without dry-out occurring. A minimum mLHP thermal resistance of 0.111 °C/W was achieved at a heat load of 11 W in the gravity-assisted operation, at which the evaporator temperature was about 97.2 °C. Huang et al. significantly reduced the manufacturing cost of LHPs through an innovative design of evaporator, making LHPs more competitive for commercial applications [19]. The cost of a 100W LHP with organic solvent as the working fluid is less than 20 USD in mass production. The LHP was successfully used in LED luminaire, solar water heater, and thermoelectric power generator for heat dissipation. More than 30,000 LHPs were manufactured and used in various products during the past 10 years. No any LHP operation failure was reported so far.

Because the LHP can realize efficient long-distance heat transfer, in the case the cooling space is remote to the heat source but is sufficient, it is feasible to create a LHP-based cooling system to transport the heat generated from the heat source to a relatively large fin radiator with no fan, where the heat is dissipated to the ambient completely in the form of natural convection. For such a cooling system, no power is consumed, and simultaneously no noise is generated, i.e., an absolutely quiet and energy-saving cooling system. Based on this idea, a LHP-based cooling system will be developed in this work, and its thermal performance mainly including the startup, heat transfer resistance and the antigravity capability will be experimentally investigated, as reported in detail below.

## **2 Experimental system**

The cooling system investigated here was mainly composed of three parts: an aluminum saddle, an ammonia-stainless steel LHP and a fin radiator, as shown in Fig. 1 (a), (b) and (c), respectively, and Fig. 2 shows an assembly of this cooling system. With the help of the saddle, heat source with a flat thermo-contact surface can be conveniently

connected to the cylindrical evaporator of the LHP. In the experiment, the heat source was simulated by a film electric resistance heater measuring 6.0×7.0 cm (L×W). The film heater was directly connected to a DC power supply, of which the power output can be adjusted continuously in a wide range of 0-1000 W with an uncertainty about 5.0%.

The LHP is the core component for this cooling system, which absorbs the heat generated from the heat source, and then efficiently transports it to a remote fin radiator. Fig. 3 shows schematically the basic structure of a LHP, consisting of an evaporator, a condenser, a compensation chamber (CC) and vapor and liquid transport lines. Fig. 4 shows the detailed internal structure of the evaporator and CC. In this work, all the components of the LHP were made of stainless steel except that the evaporator wick was made of sintered nickel powders, and ammonia was selected as the working fluid due to its excellent thermo-physical properties in the ambient temperature range of 0-60°C. Table 1 provides the basic parameters of the LHP where OD and ID represent the outer and inner diameters respectively. The condenser line was embedded into the flat bottom surface of the fin radiator with a relatively large volume measuring 35.0×20.0×3.7 cm (L×W×H), where heat dissipation to the ambient was completely in the form of natural convection. The fin radiator was made of aluminum alloy, and Table 2 provides the basic parameters of the fin radiator.

Thirteen type-T thermocouples with the maximum measurement error of  $\pm 0.5$  °C were employed to monitor the temperature profile along the loop, as illustrated in Fig. 2. Temperature data from the thermocouples was recorded, displayed and stored every five seconds by a data acquisition system (Agilent 34970A) linked to a PC. The thermocouple junction was covered by a layer of thermal insulation material to reduce the heat transfer to the ambient surroundings, so that the measured wall temperatures should be very close to the temperatures of the working fluid inside, as the wall thickness was no more than 1.0 mm for all the LHP components.

### **3 Experimental results and discussions**

### 3.1 Startup

For a LHP-based cooling system, successful startup is always the first and most important issue to be addressed prior to its practical applications. Typically, a LHP can realize self-startup without any preconditioning. However, self-startup does not mean instant startup, and the startup may take a long time accompanied by very large evaporator temperature rise, especially when the startup heat load is relatively small. As a two-phase heat transfer device, the startup of a LHP is a very complex dynamic process, ranging from the application of a heat load to the evaporator to the normal circulation of working fluid in the loop. During this process, a variety of heat transfer phenomena such as evaporation, boiling, condensation and convection may be involved, accompanied by complicated liquid/vapor movement and phase redistribution. According to previous studies, the startup of a LHP is affected by multiple factors. In particular, it is strongly influenced by the initial liquid/vapor distribution in the evaporator, and four possible startup situations have been identified, as listed in Table 3. Many experiments have shown that LHPs are the easiest to start up in situation 2, but the most difficult in situation 3 [20-25].

#### 3.1.1 Startup with different heat loads

##### 1) Startup with an input power of 2 W

Figure 5 shows the temperature changes during the startup process with an input power of 2 W. In Fig. 5, the ambient air was used as the heat sink with a constant temperature of about 24 °C, and the evaporator, CC and condenser were placed in a horizontal plane, i.e., no adverse elevation existed.

According to Fig. 5, at the initial state, all the components of the LHP remained nearly at the ambient temperature. With an electric power of 2 W applied to the film electric resistance heater, its temperature (TC1) together with the evaporator wall temperature (TC3) began to rise quickly. At the same time, TC4 at the evaporator outlet also increased slowly, indicating that some vapor should be generated in the evaporator and flowed into the vapor line. It can be inferred that vapor should exist in the vapor grooves prior to the application

of the heat load; otherwise if the vapor grooves are completely filled by liquid, a certain superheat will be needed to initiate the nucleate boiling there, causing an obvious delay of vapor generation. TC13 on the top of the CC also increased quickly following the rise of the evaporator wall temperature, indicating that the heat leak from the evaporator to the CC was relatively large. That is because liquid/vapor two-phase working fluid exists in the evaporator core, and the heat transfer from the evaporator core to the CC is in the form of evaporation and condensation, just like the process occurred in a conventional heat pipe. Therefore, this startup corresponds to the situation 4 in Table 3, i.e., vapor exists in both the vapor grooves and the evaporator core.

The evaporator wall temperature TC3 initially rose quickly, but after reaching approximately 29 °C, it began to rise very slowly until achieving a steady state. The temperatures of the film heater and the CC followed the same trend as the evaporator wall temperature. It should be of note that at the steady state, the temperature at the condenser inlet TC5 still remained at the ambient temperature, suggesting that the vapor generated in the evaporator does not enter the condenser, i.e., the condenser is completely not utilized. That is because the heat load applied to the evaporator is too small, and the mass flowrate in the loop becomes very small accordingly. To balance the heat leak from the evaporator to the CC, a large subcooling for the retuning fluid will be needed, resulting in an enhanced operating temperature of the LHP. At a high operating temperature, vapor generated in the evaporator will fully condense to liquid in the vapor line before entering the condenser.

## 2) Startup with an input power of 5 W

Figure 6 shows the temperature changes during the startup process with an input power of 5 W. In Fig. 6, the other operating conditions are all the same as those in Fig. 5. According to Fig. 6, at the initial state, all the components of the LHP remained nearly at the ambient temperature. With an electric power of 5 W applied to the film heater, its temperature (TC1) together with the evaporator wall temperature (TC3) began to rise quickly. At the same time, TC4 at the evaporator outlet also increased slowly, indicating that vapor should be generated

in the evaporator and flowed into the vapor line. It can be inferred that vapor should exist in the vapor grooves prior to the application of the heat load. TC13 on the top of the CC also increased following the rise of the evaporator wall temperature, indicating that the heat leak from the evaporator to the CC was relatively large. That is because liquid/vapor two-phase working fluid exists in the evaporator core, as analyzed above.

When the evaporator wall temperature reached about 33.5 °C, a sudden temperature drop for the film heater and evaporator wall occurred accompanied by a sudden temperature rise at the evaporator outlet and the CC. That is because some vapor grooves are completely filled by liquid, and a certain superheat is needed to initiate the nucleate boiling there. With the increase of the evaporator temperature, the liquid superheat increased until the onset of nucleate boiling in the vapor grooves filled by liquid. The temperatures of the film heater (TC1) and evaporator wall (TC3) then dropped sharply due to the absorption of heat by liquid evaporation. On the contrary, the temperatures at the evaporator outlet (TC4) and the CC (TC13) rose suddenly, indicating that the generated vapor flows along two opposite paths: some vapor enters the vapor line, while the other penetrates the wick and enters the CC due to the very high vapor pressure produced at the moment nucleate boiling occurs. Therefore, this startup corresponds to a mixture of situations 3 and 4 in Table 3, i.e., vapor exists in the evaporator core and some vapor grooves, and the other vapor grooves are completely filled by liquid.

With the pressure increase in the CC, vapor generated in the evaporator will no longer be able to penetrate the wick due to insufficient pressure difference between the evaporator and the CC. Under this condition, vapor generated in the evaporator can only flow in the positive direction, i.e., entering the vapor line and the condenser in sequence. With the normal circulation of the working fluid in the loop, the temperatures of the film heater and evaporator wall dropped gradually until reaching a steady state. It should be of note that at the steady state, the temperature at the condenser inlet TC5 was very close to the temperature at the evaporator outlet, showing that the vapor generated in the evaporator enters the condenser, and some part of the condenser is utilized, different

from the case in Fig. 5.

### 3) Startup with an input power of 10 W

Figure 7 shows the temperature changes during the startup process with an input power of 10 W. In Fig. 7, the other operating conditions are all the same as those in Fig. 5. According to Fig. 7, at the initial state, all the components of the LHP remained nearly at the ambient temperature. With an electric power of 10 W applied to the film heater, its temperature (TC1) together with the evaporator wall temperature (TC3) began to rise quickly. TC4 at the evaporator outlet remained constant, indicating that vapor was not generated in the evaporator, and the vapor grooves should be completely filled by liquid. At the same time, TC13 on the top of the CC also kept unchanged, showing that heat leak from the evaporator to the CC is very small, and the evaporator core should be completely filled by liquid. Therefore this startup corresponds to the situation 1 in Table 3.

When the evaporator wall temperature reached about 25.3 °C, a sudden temperature drop for the film heater and evaporator wall occurred accompanied by a sudden temperature rise at the evaporator outlet and the CC, very similar to the case in Fig. 6. With the normal circulation of the working fluid in the loop, the temperatures of the film heater and evaporator wall gradually reached a steady state. It should be of note that at the steady state, the temperature at the condenser TC6 was very close to the temperature at the evaporator outlet, showing that the vapor generated in the evaporator enters the condenser with a larger length compared with that in Fig. 6, i.e., the utilization efficiency of the condenser becomes larger.

### 4) Startup with an input power of 20 W

Figure 8 shows the temperature changes during the startup process with an input power of 20 W. In Fig. 8, the other operating conditions are all the same as those in Fig. 5. According to Fig. 8, at the initial state, all the components of the LHP remained nearly at the ambient temperature. With an electric power of 20 W applied to the film heater, its temperature (TC1) together with the evaporator wall temperature (TC3) began to rise quickly.

TC4 at the evaporator outlet remained constant, indicating that vapor was not generate in the evaporator immediately, and the vapor grooves should be completely filled by liquid. At the same time, TC13 on the top of the CC increased quickly following the evaporator wall temperature, showing that the heat leak from the evaporator to the CC is very large, and liquid/vapor two phase working fluid should exist in the evaporator core. Therefore this startup corresponds to the situation 2 in Table 3, which is the most difficult to realize the startup.

When the evaporator wall temperature reached about 35 °C, a sudden temperature drop for the film heater and evaporator wall occurred accompanied by a sudden temperature rise at the evaporator outlet and the condenser inlet. That was because nucleate boiling occurred in the vapor grooves, which absorbed the heat from the film heater and the evaporator wall, and the generated vapor flowed into the vapor line and the condenser in sequence. With the normal circulation of the working fluid in the loop, the temperatures of the film heater and evaporator wall dropped gradually until reaching a steady state. It should be of note that at the steady state, the temperature at the condenser outlet TC11 was very close to the temperature at the evaporator outlet, indicating that the vapor generated in the evaporator almost fully occupied the condenser, and the utilization efficiency of the condenser nearly reached its maximum under this condition.

### 3.1.2 Startup with temperature oscillation

For two-phase heat transfer devices, operating instability is a common phenomenon, which seems inevitable to occur. For LHPs, typical operating instability phenomena such as temperature oscillation, temperature hysteresis, and working fluid reverse flow during LHP startup or operation have been reported [26-28]. To date, some relevant studies on the temperature oscillation in LHP operation have been conducted [29-32], and several reasons have been presented: a) it is found that when the vapor front moves near the inlet or outlet of the condenser, the vapor front may not be able to find a stable location, and will move back and forth around these locations, causing periodic temperature oscillations of the LHP components. Some researchers ascribed it to

inappropriate working fluid inventory or the variation of vapor void fraction in the evaporator core. (b) When a large thermal mass is attached to the evaporator, under some conditions, the thermal mass can modulate the constant applied input power into an oscillatory one to the evaporator, and the oscillatory evaporator power becomes the source of the temperature oscillation.

For this cooling system, when the input power was 20 W, an obvious temperature oscillation was also observed during the startup process, and finally the cooling system maintained a temperature-oscillating operation, as illustrated in Fig. 9. In Fig. 9, according to the analysis in section 3.1.1 above, when an input power of 20 W was applied to the film heater, the LHP began to start up in situation 2, which is the most favorable condition for startup. However, after the film heater and evaporator wall temperatures maintained stable for only a couple of minutes, they began to rise quickly, reaching a peak value, and then began to drop quickly to the valley value. After maintaining the valley value for only a couple of minutes, they began to rise again, and formed a quasi-periodic temperature change. It is found that when the evaporator wall and CC temperatures were at their peak values, the temperature at the CC inlet was at the lowest value. Because the subcooling degree for the returning liquid was so large that it would inevitably cause the subsequent temperature drop for the evaporator and the CC. When the evaporator wall temperature dropped to its valley value, the condenser was almost fully utilized, and the temperature at the condenser outlet (TC11) became very close to the vapor temperature at the evaporator outlet. Under this condition, the liquid temperature at the CC inlet increased sharply to approach approximately the vapor temperature. Since the subcooling degree for the returning liquid at the CC inlet decreased to a minimum value, and the return subcooling cannot balance the heat leak from the evaporator to the CC, the temperatures for the evaporator and the CC would rise again. Based on the analysis above, the temperature oscillation was closely associated the energy imbalance of the CC, i.e., excessive return subcooling resulted in the temperature drop for the evaporator and the CC, while insufficient return subcooling led to their temperature

rise. However, to reveal clearly in what situation this temperature oscillation will occur and why the temperature oscillation can always last, a more in-depth study is really needed.

## 3.2 Power increment test

### 3.2.1 Operation under horizontal orientation

Figure 10 shows the temperature changes of some key points along the loop during the power increment test, where the ambient air was used as the heat sink with a constant temperature of about 23 °C, and the evaporator, CC and condenser were placed in a horizontal plane, i.e., no adverse elevation existed.

According to Fig. 10, when the input power to the film heater was increased from 30 to 60 W, the steady-state operating temperature of the evaporator wall first dropped from 46.0 to 38.2 °C; while when the input power was increased from 60 to 150 W gradually with an interval of 30 W, the evaporator wall temperature always kept increasing. The film heater temperature followed the same variation trend as that of the evaporator wall, but the temperature difference between them increased almost linearly with the increasing input power. At the maximum input power of 150 W, the film heater reached the highest temperature of about 76.3 °C.

An impressive result can be observed at the input power of 120 W in Fig. 10, i.e., the maximum temperature difference along the entire loop (~4.6 meter long, excluding the film heater temperature) reached a minimum value of about 5.0 °C, indicating that the LHP studied here possessed very good manufacture quality and exhibited very excellent heat transfer performance. While there have been many parameters to assess the operating performance of a LHP, in the authors' opinion, the maximum temperature difference along the entire loop can be considered as the most basic one, which can directly reflect the temperature uniformity along the entire loop. The smaller the maximum temperature difference along the entire loop, the better the LHP performance. Although based on the fundamental principle of LHP operation, a temperature difference along the loop is necessary to realize the energy balance for each component of the LHP, this temperature difference should

be reduced as much as possible to enhance the overall performance of the LHP.

Generally, in the steady-state operation, a relatively large subcooling degree for the returning liquid at the CC inlet ( $\Delta T_{sub}$ ) is required to balance the heat leak from the evaporator to the CC ( $Q_{hl}$ ), as shown by equation (1):

$$Q_{hl} = Q_{sub} = \dot{m}_{pl} c_{pl} \Delta T_{sub} = \dot{m}_{pl} c_{pl} (T_{CC,in} - T_{CC}) \quad (1)$$

According to equation (1), the larger the heat leak from the evaporator to the CC, the greater the subcooling degree is required. Typically, the heat leak from the evaporator to the CC is determined by a variety of factors such as the input power, the length and diameter of the transport lines, the length and diameter of the condenser, the size and material of the evaporator casing, and the size and material of the evaporator wick. Besides these factors, the sealing quality between the evaporator and the CC is also a very important influencing factor. If the sealing quality is not very good, and even a small amount of vapor generated at the outer surface of the wick enters the CC, it will cause significantly increased heat leak from the evaporator to the CC accompanied by very large subcooling degree at the CC inlet and maximum temperature difference along the entire loop. That is because the evaporative latent heat of the working fluid is generally very large, leading to a relatively large heat leak from the evaporator to the CC compared with those through thermal conduction and convection in the radial and axial direction of the evaporator, as shown by equation (2):

$$Q_{hl,v} = \dot{m}_v h_{fg} \quad (2)$$

Even the sealing quality is very good, i.e., no vapor generated at the outer surface of the wick enters the CC directly, because at a small input power, the mass flowrate of the working fluid in the loop is so small that a large subcooling degree for the liquid at the CC inlet is also required. For instance, in Fig. 10, when the input power was 30 W, the subcooling degree for the liquid at the CC inlet reached as large as 23.3 °C, and the maximum temperature difference along the entire loop reached about 26.0 °C.

### 3.2.2 Operation with adverse elevation

Figures 11 and 12 show the temperature changes of some key points along the loop during the power increment test, where the operating conditions were all the same as those in Fig. 10 except that the adverse elevation was 0.3 and 0.5 m respectively, i.e., the evaporator was placed 0.3 and 0.5 m higher than the condenser, respectively in the experiment.

From Figs. 11 and 12, it is found that the LHP can operate normally with an adverse elevation of 0.3 or 0.5 m, exhibiting a very strong and robust capability of antigravity operation, which is one of the main advantages for LHPs over conventional heat pipes. While for traditional heat pipes, the antigravity capability is very weak, i.e., typically on the level of millimeter or centimeter, and a small increase in the adverse elevation will cause an obvious performance degradation. In some particular applications, the heat pipes have to be designed to operate at an antigravity orientation [33-35]. Under this condition, the normal operation of the heat pipes will be at the expense of significantly reduced heat transfer capacity, where the limited capillary pressure has to overcome both the liquid frictional pressure drop and the gravitational pressure drop.

Comparing Figs. 11 and 12 with Fig. 10, it is found that although the LHP can operate normally with the presence of adverse elevation, the evaporator wall temperature becomes obviously higher at small input powers. For instance, when the input power was 30 W, the evaporator wall temperature at the steady state was about 46.2 °C under the horizontal orientation; however, it was increased to about 52.0 and 55.6 °C corresponding to an adverse elevation of 0.3 and 0.5 m respectively, as shown in Fig. 13. That is because the existence of adverse elevation will produce an additional gravitational pressure drop, as shown by equation (3):

$$\Delta P_g = \rho_l g H_g \quad (3)$$

According to the Clausius-Clapeyron equation, an increase in the total pressure drop along the external loop will cause an increase in the temperature difference between the evaporator and the CC, as shown by equation (4):

$$\Delta T_{e-cc} = \left( \frac{dT}{dP} \right)_{sat} \times \Delta P_{ext} = \left( \frac{T v_{fg}}{h_{fg}} \right)_{sat} \times (\Delta P_f + \Delta P_g) \quad (4)$$

Under this condition, the heat leak from the evaporator to the CC increases due to the presence of the adverse elevation, and the larger the adverse elevation, the greater the heat leak from the evaporator to the CC. To balance the increased heat leak from the evaporator to the CC due to the presence of the adverse elevation, a larger subcooling degree for the returning liquid at the CC inlet is required, and the subcooled zone in the condenser must be enlarged accordingly. As a result, the two-phase zone in the condenser reduces, leading to a decreased utilization efficiency of the condenser and an increased operating temperature of the LHP eventually. At relatively high input powers, i.e.,  $\geq 120$  W, the effect of adverse elevation on the evaporator wall temperature becomes insignificant, which can be generally neglected. That is because the mass flowrate of the working fluid in the loop increases almost linearly with the increasing input power, and under this condition, the increase in the heat leak from the evaporator to the CC due to the presence of the adverse elevation can be easily balanced by the subcooling of the returning liquid without an obviously increased subcooling degree. Therefore, the presence of adverse elevation will not cause notable temperature changes at the key points along the loop, as shown in Figs. 11 and 12.

### 3.3 System thermal resistance

Figure 14 shows the variation of the system thermal resistance of the LHP-based cooling system with the increase of the input power. In this work, the system thermal resistance is defined as the heat source to heat sink thermal resistance, which can be expressed by equation (5):

$$R_{\text{sys}} = \frac{T_{\text{source}} - T_{\text{sink}}}{Q_{\text{ap}}} \quad (5)$$

According to Fig. 14, when the LHP was operating under the horizontal orientation, with the increase of the input power, the system thermal resistance first dropped quickly from an initial 1.12 °C/W at an input power of 30 W, then it began to drop very slowly and gradually reached an almost constant value of about 0.30 °C/W from the input power of 120 W. This result is closely associated with the unique operating characteristics of LHPs,

where there exists two operating modes for LHP operation, i.e., the variable conductance mode and the constant conductance mode. When the input power is relatively small, the LHP is operating in the variable conductance mode, and the utilization efficiency of the condenser increases gradually with increasing input power, leading to a continuously reduced system thermal resistance. When the condenser utilization efficiency reaches its maximum value, the LHP will operate in the constant conductance mode, and under this condition, the system thermal resistance will maintain an almost constant value. When the LHP was operating with an adverse elevation of 0.3 or 0.5 m, the system thermal resistance exhibited very similar variation trends to that under horizontal orientation, except that the system thermal resistance was obviously higher at small input powers, which is in agreement with the results in Fig. 13.

## 4 Conclusions

In this work, a LHP-based cooling system was developed and tested, which featured no power consumption and no noise. Extensive experimental studies were carried out mainly focusing on the startup characteristics and system thermal resistance. Based on the experimental results and analysis, some important conclusions have been drawn, as summarized below:

- At small input powers, the LHP-based cooling system can successfully realize the startup, and maintain the stable operation. The LHP-based cooling system may start up in different situations, and sometimes even in a mixture of two situations, where the key points along the loop exhibit quite different temperature variation characteristics.
- Startup with obvious temperature oscillation is observed for this LHP-based cooling system, which is closely associated with the energy imbalance of the CC, i.e., excessive return subcooling leads to the evaporator temperature rise, while insufficient return subcooling results in the temperature drop.
- With the film heater temperature not exceeding 80 °C, this cooling system can dissipate a heat load up to 150

W to the ambient at a temperature about  $24\text{ }^{\circ}\text{C}$  over a transport distance of 1.05 m.

- This cooling system exhibits very strong antigravity capability. With an adverse elevation of 0.5 m, the cooling system can maintain normal operation, and no obvious performance decay appears except an increased operating temperature at small input powers.
- For the LHP-based cooling system, the system thermal resistance first drops quickly, then it begins to drop very slowly and gradually reaches an almost constant value of about  $0.30\text{ }^{\circ}\text{C}/\text{W}$ .

### **Acknowledgements**

This work was supported by the Beijing Natural Science Foundation (No. 3182023), National Natural Science Foundation of China (Nos. 51576010 and 51776012).

## References

- [1] S. M. Sohel Murshed, C. A. Nieto de Castro, A critical review of traditional and emerging techniques and fluids for electronics cooling, *Renewable and Sustainable Energy Reviews*, 78 (2017) 821-833
- [2] Mehdi Bahiraei, Saeed, Heshmatian, Electronics cooling with nanofluids: A critical review, *Energy Conversion and Management*, 172 (2018) 438-456
- [3] Ali C. Kheirabadi, Dominic Groulx, Cooling of server electronics: A design review of existing technology, *Applied Thermal Engineering*, 105 (2016) 622-638
- [4] Ali C. Kheirabadi, Dominic Groulx, Experimental evaluation of a thermal contact liquid cooling system for server electronics, *Applied Thermal Engineering*, 129 (2018) 1010-1025
- [5] Burt S. Tilley, On microchannel shapes in liquid-cooled electronics applications, *International Journal of Heat and Mass Transfer*, 62 (2013) 163-173
- [6] I. Gabsi, S. Maalej, M. C. Zaghdoudi, Thermal performance modeling of loop heat pipes with flat evaporator for electronics cooling, *Microelectronics Reliability*, 84 (2018) 37-47
- [7] Jiazheng Lu, Limei Shen, Qingjun Huang, et al., Investigation of a rectangular heat pipe radiator with parallel heat flow structure for cooling high-power IGBT modules, *International Journal of Thermal Sciences*, 135 (2019) 83-93
- [8] Chengdi Xiao, Qing Tian, Can Zhou, A novel cooling system based on heat pipe with fan for thermal management of high-power LEDs, *J. Opt.* 46 (2017) 269–276
- [9] Ying-Che Weng, Hung-Pin Cho, Chih-Chung Chang, Heat pipe with PCM for electronic cooling, *Applied Energy*. 88 (2011) 1825–1833
- [10] Thanh-Ha Tran, Souad Harmand, Bernard Sahut, Experimental investigation on heat pipe cooling for Hybrid Electric Vehicle and Electric Vehicle lithium-ion battery, *J. Power Sources*. 265 (2014) 262–272
- [11] Y. F. Maydanik, Loop heat pipes, *Applied Thermal Engineering*, 25 (2005) 635–657
- [12] J. Ku, Operating Characteristics of Loop Heat Pipes, SAE Paper, No. 1999-01-2007, 1999
- [13] Jiang He, Guiping Lin, Lizhan Bai, et al., Effect of non-condensable gas on the operation of a loop heat pipe. *International Journal of Heat and Mass Transfer* 70(2014) 449-462
- [14] Y. Maydanik, V. Pastukhov, M. Chernysheva, Development and investigation of a loop heat pipe with a high heat-transfer capacity, *Applied Thermal Engineering* 130 (2018) 1052-1061
- [15] V.S. Jasvanth, Abhijit A. Adoni, V. Jaikumar, et al., Design and testing of an ammonia loop heat pipe, *Applied Thermal Engineering* 111 (2017) 1655-1663

- [16] V. G. Pastukhov, Yu. F. Maidanik, C. V. Vershinin, et al., Miniature Loop Heat Pipes for Electronics Cooling, *Appl. Thermal Eng.* 23 (2003) 1125–1135.
- [17] V. G. Pastukhov, Y. F. Maydanik, Low-noise cooling system for PC on the base of Loop Heat Pipes. *Applied Thermal Engineering*, 27(2007), 894-901
- [18] Guohui Zhou, Ji Li, Lucang Lv, An ultra-thin miniature loop heat pipe cooler for mobile electronics, *Applied Thermal Engineering* 109 (2016) 514–523
- [19] Bin-Juine Huang, Yi-Hung Chuang, Po-En Yang, Low-cost manufacturing of loop heat pipe for commercial applications, *Applied Thermal Engineering* 126 (2017) 1091–1097
- [20] Wukchul Joung, Taeu Yu, Jinho Lee, Experimental study on the operating characteristics of a flat bifacial evaporator loop heat pipe, *International Journal of Heat and Mass Transfer* 53( 2010) 276–285
- [21] Randeep Singh, Aliakbar Akbarzadeh, Masataka Mochizuki, Operational characteristics of the miniature loop heat pipe with non-condensable gases, *International Journal of Heat and Mass Transfer* 53(2010) 3471–3482
- [22] M. N. Nikitkin, W. B. Bienert, K. A. Goncharov, Non-condensable gases and loop heat pipe operation, SAE Paper, No. 981584, 1998
- [23] Kimberly R. Wrenn, David A. Wolf, Edward J. Krolczek, Effect of noncondensable gas and evaporator mass on loop heat pipe performance. SAE Paper, No. 2000-01-2409, 2000
- [24] H. X. Zhang, G. P. Lin, T. Ding, et al, Investigation of startup behaviors of a loop heat pipe, *Journal of Thermophysics and Heat Transfer*, 19(4)(2005) 509-518
- [25] T. T. Hoang, R. W. Baldauff, K. H. Cheung, Start-up behavior of an ammonia loop heat pipe, AIAA paper, No. 2005-5630
- [26] Jianting Feng, Guiping Lin, Lizhan Bai, Experimental investigation on operating instability of a dual compensation chamber loop heat pipe, *Science in China Series E: Technological Sciences* 52(8)( 2009) 2316-2322
- [27] Yuming Chen, Manfred Groll, Rainer Mertz, et al. Steady-state and transient performance of a miniature loop heat pipe. *International Journal of Thermal Sciences* 45 (2006) 1084–1090
- [28] Tarik Kaya, Jentung Ku. Thermal Operational Characteristics of a Small-Loop Heat Pipe. *Journal of Thermophysics and Heat Transfer* 17(4)(2003) 464-470
- [29] S.V. Vershinin, Yu.F. Maydanik. Investigation of pulsations of the operating temperature in a miniature loop heat pipe. *International Journal of Heat and Mass Transfer* 50 (2007) 5232–5240

- [30] Xianfeng Zhang, Jiepeng Huo, Shuangfeng Wang. Experimental investigation on temperature oscillation in a miniature loop heat pipe with flat evaporator. *Experimental Thermal and Fluid Science* 37 (2012) 29–36
- [31] Randeep Singh, Aliakbar Akbarzadeh, Masataka Mochizuki. Operational characteristics of a miniature loop heat pipe with flat evaporator. *International Journal of Thermal Sciences* 47 (2008) 1504–1515
- [32] Ji Li, Daming Wang, G.P. Peterson. Experimental studies on a high performance compact loop heat pipe with a square flat evaporator. *Applied Thermal Engineering* 30 (2010) 741–752
- [33] Trijo Tharayil, Lazarus Godson Asirvatham, Catrina Frances Milne Cassie, et al., Performance of cylindrical and flattened heat pipes at various inclinations including repeatability in anti-gravity-A comparative study. *Applied Thermal Engineering* 122(2017) 685–696
- [34] Hui Li, Bo Zhou, Yong Tang, et al., Effect of working fluid on heat transfer performance of the anti-gravity loop-shaped heat pipe. *Applied Thermal Engineering* 88 (2015) 391–397
- [35] Zilong Deng, Yi Zheng, Xiangdong Liu, et al., Experimental study on thermal performance of an anti-gravity pulsating heat pipe and its application on heat recovery utilization. *Applied Thermal Engineering* 125 (2017) 1368–1378

**Table captions**

Table 1 Basic parameters of the tested LHP

Table 2 Basic parameters of the fin radiator

Table 3 Liquid/vapor distribution in the evaporator

## Figure captions

Fig. 1 Components of the LHP-based cooling system

Fig. 2 Assembly of the LHP-based cooling system and thermocouple locations

Fig. 3 Basic structure of a loop heat pipe (not to scale)

Fig. 4 Detailed internal structure of the evaporator and CC of a LHP

Fig. 5 Startup with an evaporator heat load of 2 W at a horizontal orientation

Fig. 6 Startup with an evaporator heat load of 5 W at a horizontal orientation

Fig. 7 Startup with an evaporator heat load of 10 W at a horizontal orientation

Fig. 8 Startup with an evaporator heat load of 20 W at a horizontal orientation

Fig. 9 Temperature oscillation in the startup with an evaporator heat load of 20 W

Fig. 10 Temperature change with step increase of evaporator heat load at a horizontal orientation

Fig. 11 Temperature change with step increase of evaporator heat load with 0.3 m adverse elevation

Fig. 12 Temperature change with step increase of evaporator heat load with 0.5 m adverse elevation

Fig. 13 Effect of adverse elevation on the evaporator wall temperature

Fig. 14 Effect of adverse elevation on the total thermal resistance

Table 1 Basic parameters of the tested LHP

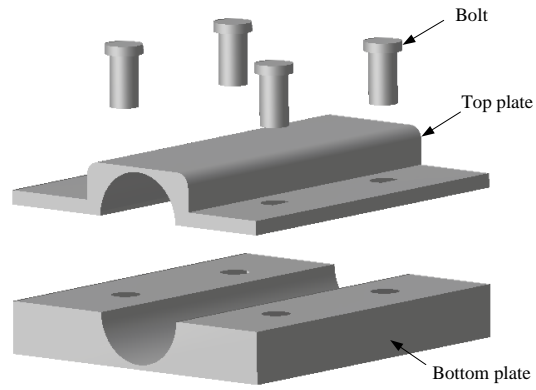
Components	Parameters
OD/ID×Length of evaporator/mm	18/16×136
OD/ID×Length of wick/mm	16/5×100
OD/ID×Length of vapor line/mm	3/2×1050
OD/ID×Length of condenser/mm	3/2×2500
OD/ID×Length of liquid line/mm	3/2×1050
Number×height×width of Grooves/mm	8×1×1
Volume of CC /ml	24.6
Working fluid inventory/g	28.2
Porosity of wick	55.0%
Maximum pore radius of wick/ $\mu\text{m}$	0.53

Table 2 Basic parameters of the fin radiator

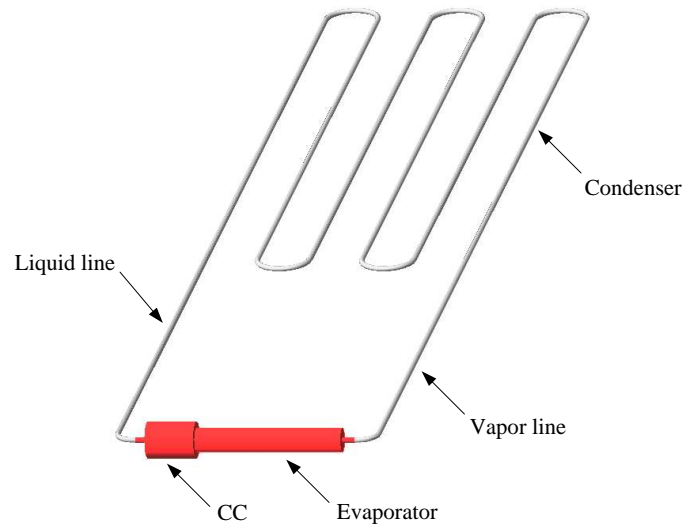
Items	Parameters
Length×Width×Height of fin radiator /mm	350×200×42
Length×Height×Thickness of fins/mm	350×35×1.5
Number×Spacing between the fins/mm	34×4.3
Number of fins	35

Table 3 Liquid/vapor distribution in the evaporator

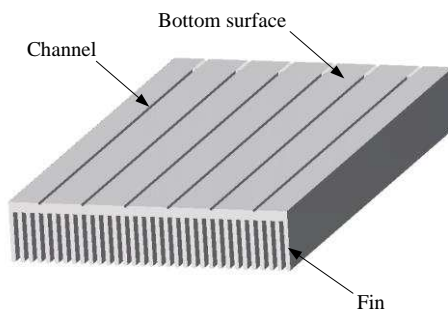
Situations	Vapor grooves/evaporator core
1	Liquid filled/liquid filled
2	Vapor exists/ liquid filled
3	Liquid filled /vapor exists
4	Vapor exists/vapor exists



(a) Saddle



(b) Loop heat pipe



(c) Fin radiator

Fig. 1 Components of the LHP-based cooling system

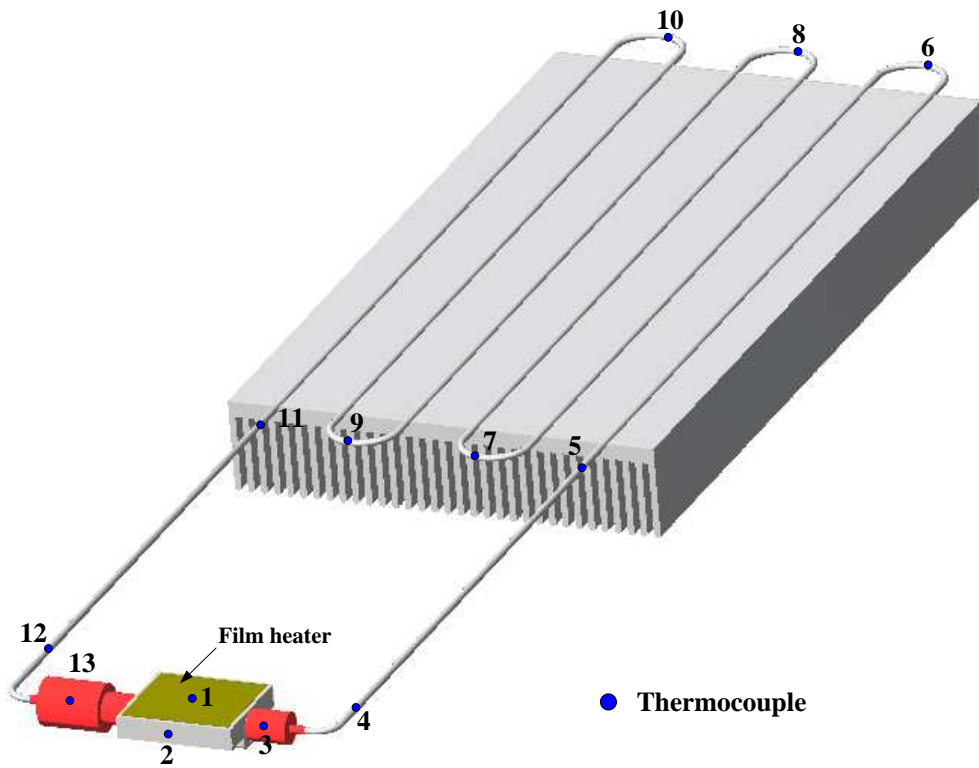


Fig. 2 Assembly of the LHP-based cooling system and thermocouple locations

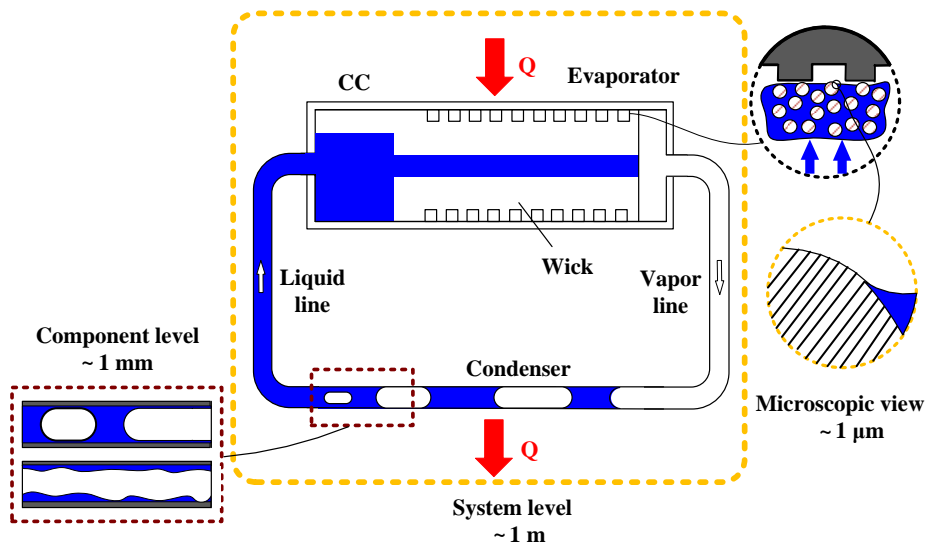


Fig. 3 Basic structure of a loop heat pipe (not to scale)

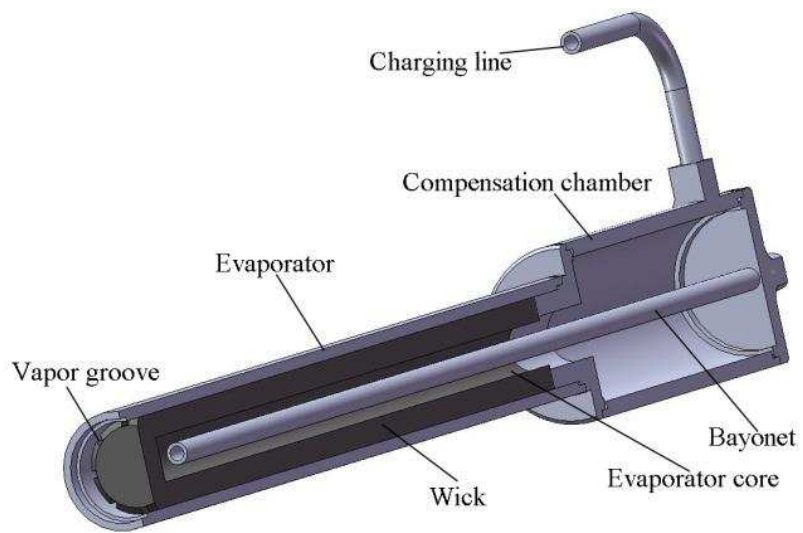


Fig. 4 Detailed internal structure of the evaporator and CC of a LHP

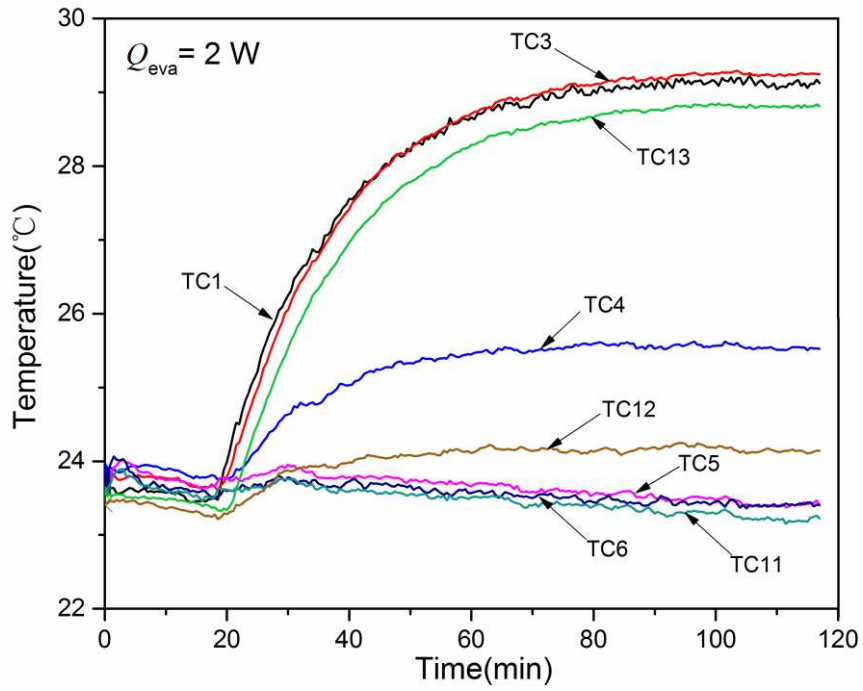


Fig. 5 Startup with an evaporator heat load of 2 W at a horizontal orientation

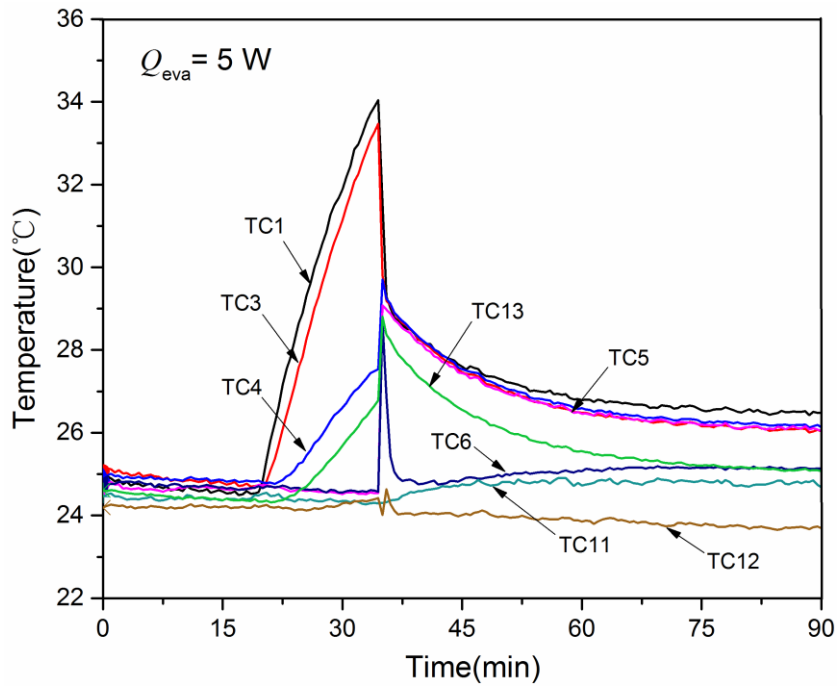


Fig. 6 Startup with an evaporator heat load of 5 W at a horizontal orientation

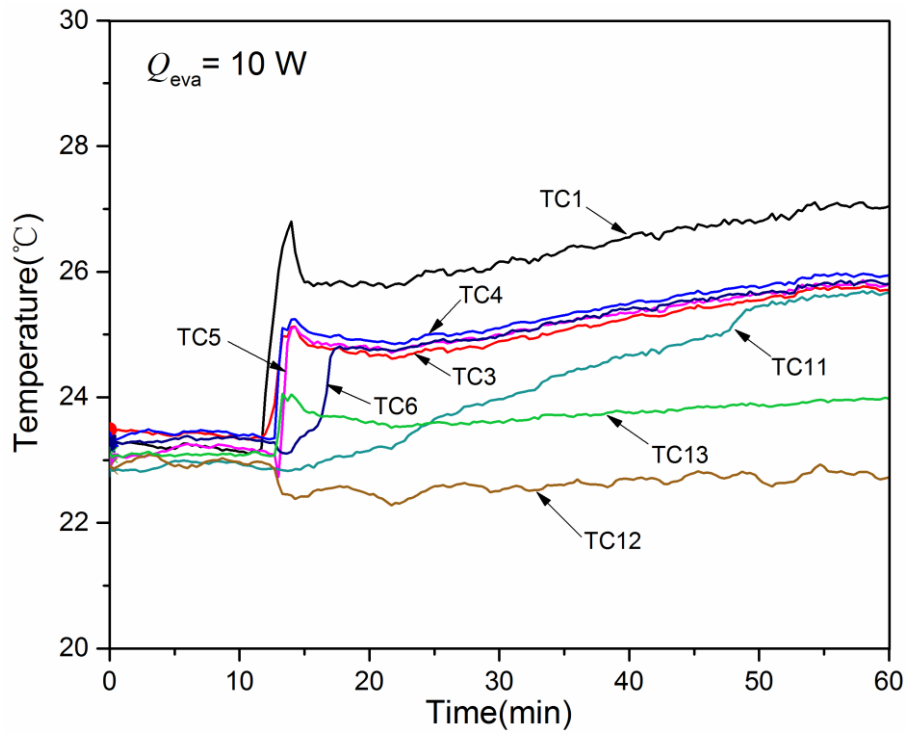


Fig. 7 Startup with an evaporator heat load of 10 W at a horizontal orientation

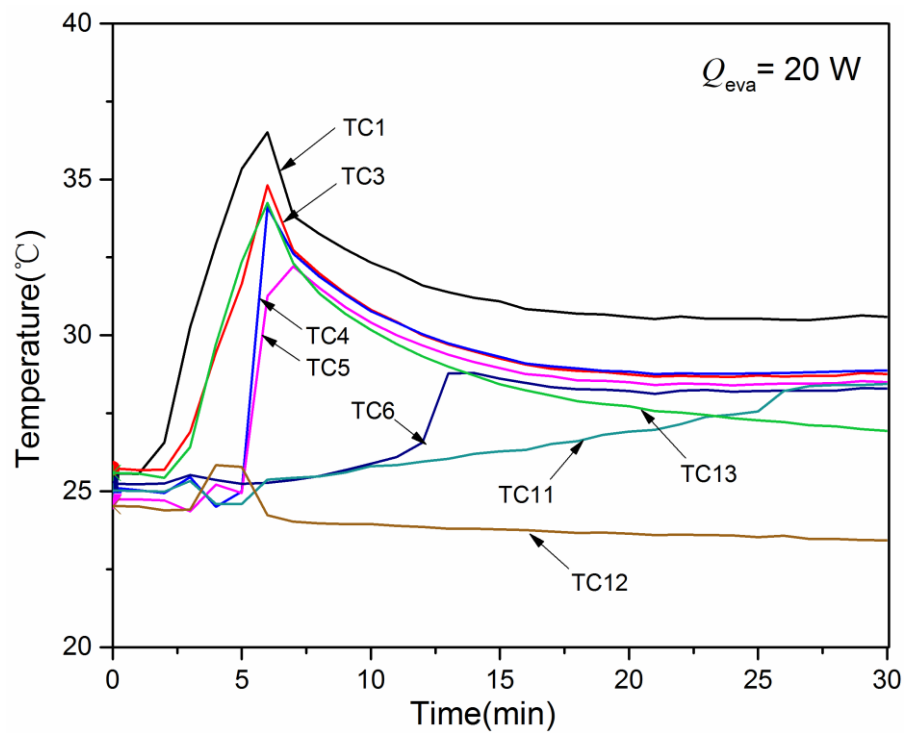


Fig. 8 Startup with an evaporator heat load of 20 W at a horizontal orientation

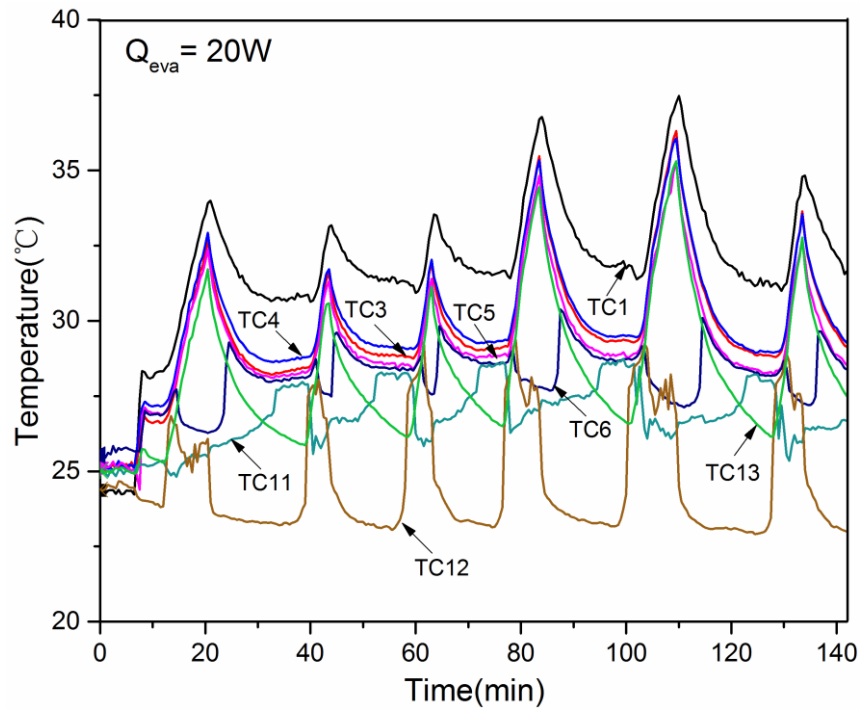


Fig. 9 Temperature oscillation in the startup with an evaporator heat load of 20 W

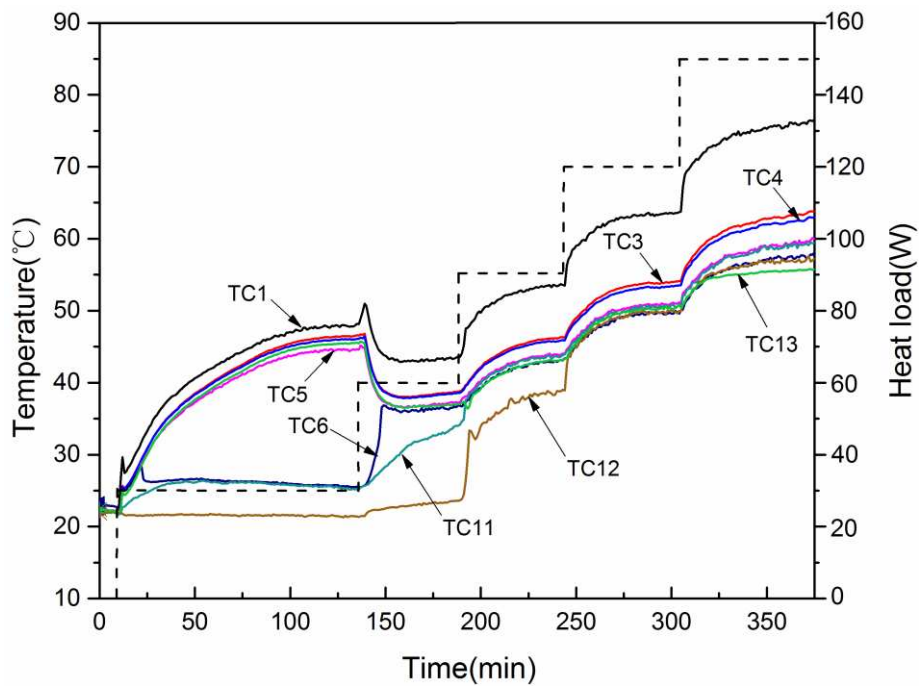


Fig. 10 Temperature change with step increase of evaporator heat load at a horizontal orientation

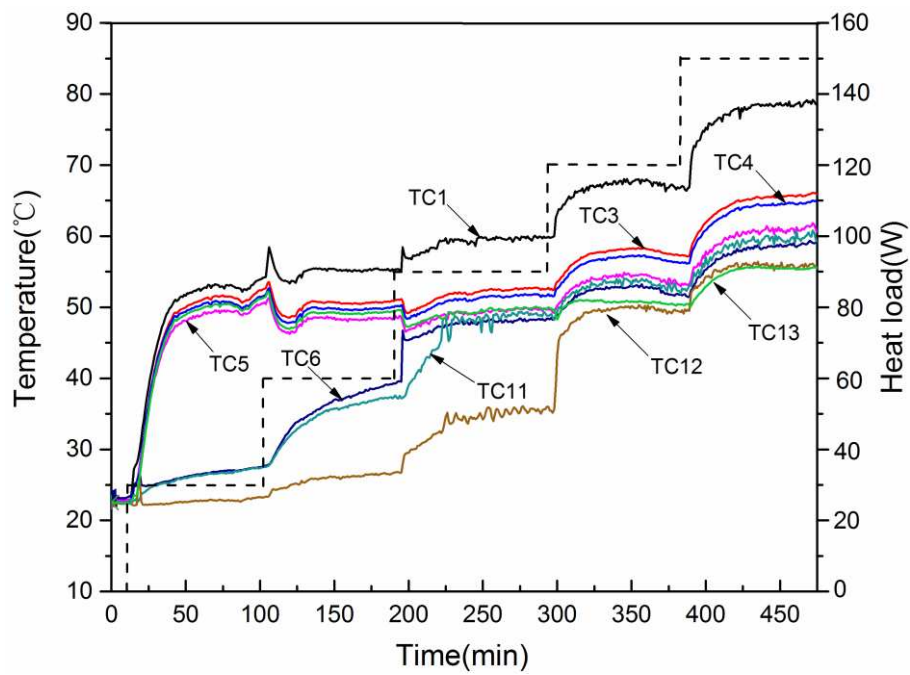


Fig. 11 Temperature change with step increase of evaporator heat load with 0.3 m adverse elevation

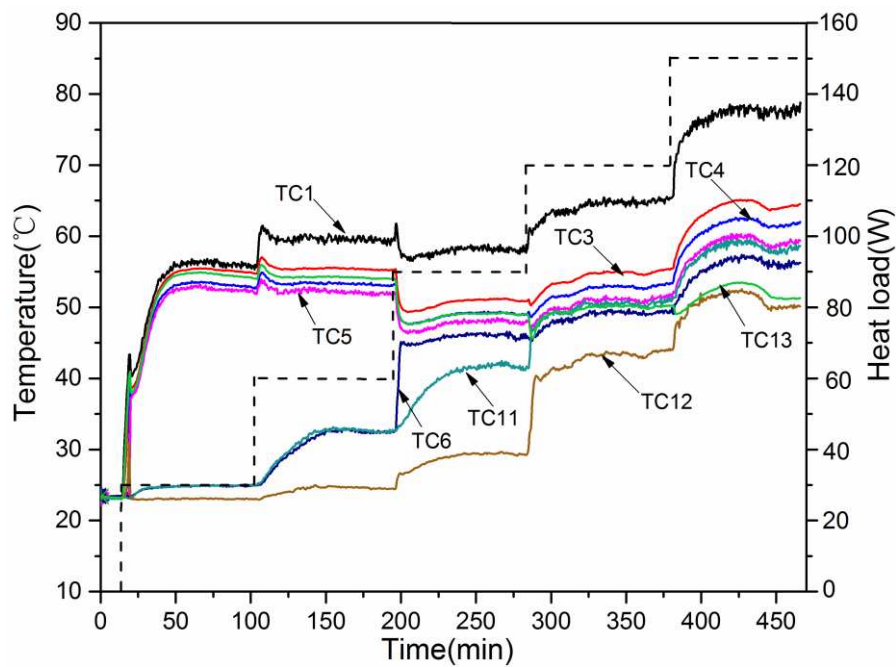


Fig. 12 Temperature change with step increase of evaporator heat load with 0.5 m adverse elevation

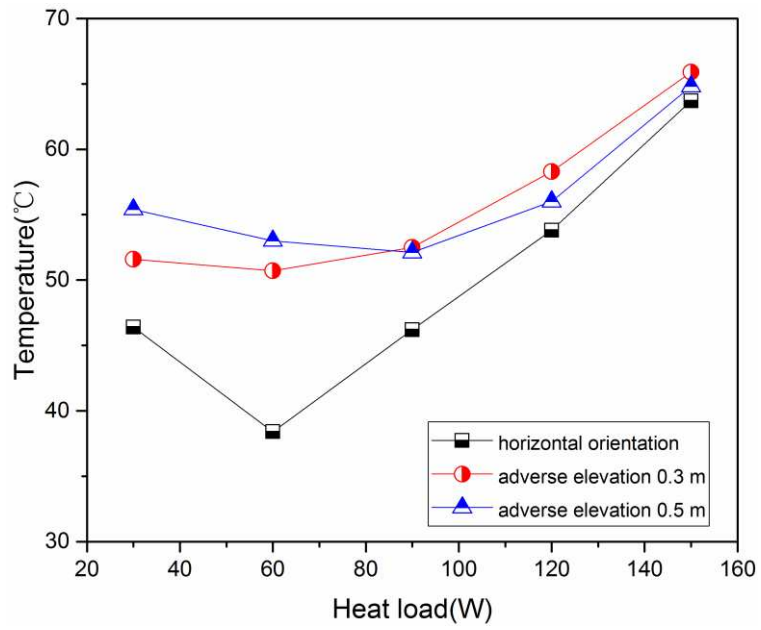


Fig. 13 Effect of adverse elevation on the evaporator wall temperature

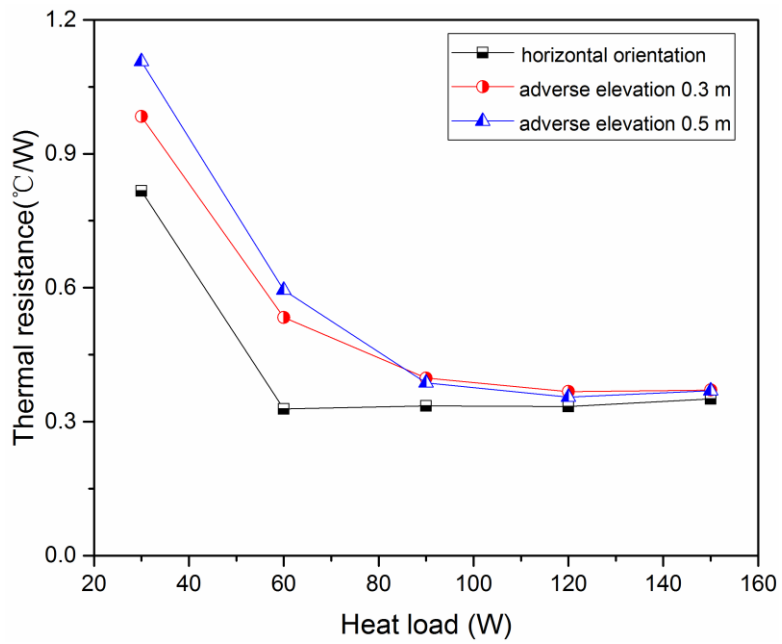


Fig. 14 Effect of adverse elevation on the total thermal resistance